BJP British Journal of Pharmacology

DOI:10.1111/bph.13109
www.brjpharmacol.org

RESEARCH PAPER

Annexin A1 mimetic peptide controls the inflammatory and fibrotic effects of silica particles in mice

P G Trentin[1]*, T P T Ferreira[1]*, A C S Arantes[1], B T Ciambarella[1], R S B Cordeiro[1], R J Flower[2], M Perretti[2], M A Martins[1] and P M R Silva[1]

[1]*Laboratory of Inflammation, Oswaldo Cruz Institute, FIOCRUZ, Rio de Janeiro, Brazil, and* [2]*Department of Biochemical Pharmacology, The William Harvey Research Institute, Queen Mary University of London, London, UK*

Correspondence
Dr Patricia M R Silva, Laboratory of Inflammation, Oswaldo Cruz Institute, FIOCRUZ, Av. Brasil 4365, Manguinhos, Rio de Janeiro, RJ 21045-900, Brazil.
E-mail: patsilva1910@gmail.com

*These authors contributed equally.

Received
15 June 2014
Revised
14 October 2014
Accepted
4 February 2015

BACKGROUND AND PURPOSE

Endogenous glucocorticoids are pro-resolving mediators, an example of which is the endogenous glucocorticoid-regulated protein annexin A1 (ANXA1). Because silicosis is an occupational lung disease characterized by unabated inflammation and fibrosis, in this study we tested the therapeutic properties of the N-terminal ANXA1-derived peptide annexin 1-(2-26) (Ac2-26) on experimental silicosis.

EXPERIMENTAL APPROACH

Swiss-Webster mice were administered silica particles intranasally and were subsequently treated with intranasal peptide Ac2-26 (200 μg per mouse) or dexamethasone (25 μg per mouse) for 7 days, starting 6 h post-challenge. Ac2-26 abolished the leukocyte infiltration, collagen deposition, granuloma formation and generation of pro-inflammatory cytokines evoked by silica; these variables were only partially inhibited by dexamethasone.

KEY RESULTS

A clear exacerbation of the silica-induced pathological changes was observed in ANXA1 knockout mice as compared with their wild-type (WT) littermate controls. Incubation of lung fibroblasts from WT mice with Ac2-26 *in vitro* reduced IL-13 or TGF-β-induced production of CCL2 (MCP-1) and collagen, but this peptide did not affect the production of CCL2 (MCP-1) by stimulated fibroblasts from formyl peptide receptor type 1 (FPR1) knockout mice. Ac2-26 also inhibited the production of CCL2 (MCP-1) from fibroblasts of FPR2 knockout mice.

CONCLUSIONS AND IMPLICATIONS

Collectively, our findings reveal novel protective properties of the ANXA1 derived peptide Ac2-26 on the inflammatory and fibrotic responses induced by silica, and suggest that ANXA1 mimetic agents might be a promising strategy as innovative anti-fibrotic approaches for the treatment of silicosis.

Abbreviations

α-SMA, α-smooth muscle actin; ANXA1, annexin A1; FPR, formyl peptide receptor; Ac2-26, annexin 1-(2-26) (peptide Ac-AMVSEFLKQAWFIENEEQEYVQTVK)

Tables of Links

TARGETS
FPR1
FPR2

LIGANDS		
Annexin 1-(2-26) (Ac2-26)	CXCL2 (MIP-2α)	IL-13
ANXA1	Dexamethasone	Methacholine
CCL2 (MCP-1)	IFN-γ	TGF-β
CXCL1 (KC)		TNF-α

These Tables list key protein targets and ligands in this article which are hyperlinked to corresponding entries in http://www.guidetopharmacology.org, the common portal for data from the IUPHAR/BPS Guide to PHARMACOLOGY (Pawson *et al.*, 2014) and are permanently archived in the Concise Guide to PHARMACOLOGY 2013/14 (Alexander *et al.*, 2013).

Introduction

Silicosis is a lung occupational disease caused by inhalation of free crystalline silica particles over a prolonged period of time. This disease mainly affects workers in the ceramic industry, glass manufacturing, sandblasting, mining, quarrying and civil construction (Leung *et al.*, 2012; Singer *et al.*, 2012). Silicosis is a problem worldwide, but it is prevalent in countries of low and middle income. China had more than 500 000 cases recorded between 1991 and 1995, and 6000 new cases and more than 24 000 deaths are reported annually (Leung *et al.*, 2012). In Brazil more than 4500 workers were reported to have silicosis between 1978 and 1998, especially in the gold-mining area in Minas Gerais (Carneiro *et al.*, 2006).

The irritative action of silica in the lungs results in the formation of nodular lesions, which may coalesce resulting in massive areas of fibrous tissue and reduction of lung elasticity (Davis, 1986). Because of its surface properties, crystalline silica leads to activation of alveolar macrophages [acting on 'scavenger' receptors such as the MARCO (macrophage receptor with collagenous structure)], epithelial cells and fibroblasts (Mossman and Churg, 1998; Fubini and Hubbard, 2003; Huaux, 2007). The granulomatous inflammation induced by silica is characterized by the accumulation of macrophages with evident presence of mineral particles in the nodules. The activation of macrophages by the ingestion of silica particles releases fibrogenic and inflammatory cytokines, which in turn stimulate lung fibroblasts to produce collagen. This ultimately leads to the development of fibrosis (Mariani *et al.*, 1996; Mossman and Churg, 1998). The inflammatory response is followed by fibrosis with the pivotal involvement of lung fibroblasts, which proliferate and produce extracellular matrix including interstitial collagen, laminin and fibronectin (Ferreira *et al.*, 2013). Once the fibrosis has developed, there is no cure and the only the clinical approach is to manage the symptoms.

It is now appreciated that the acute inflammatory response is tightly regulated by an ever-increasing group of endogenous anti-inflammatory and pro-resolving mediators, the prototype of which is cortisol (Gilroy *et al.*, 2004; Serhan, 2011). These anti-inflammatory mediators may act at different phases of the inflammatory response, blocking white cell recruitment, promoting apoptosis and stimulating phagocytosis of apoptotic cells. There are quite few examples of anti-inflammatory agents, and one of these is the glucocorticoid-regulated 37 kDa protein named annexin A1 (ANXA1) (Perretti and Gavins, 2003; Kamal *et al.*, 2005). ANXA1 is the first characterized member of the family of proteins that binds to membrane phospholipids through a calcium-dependent manner and promotes inhibition of PLA_2 and eicosanoid synthesis (Gerke *et al.*, 2005). ANXA1 is present, predominantly, in differentiated cells and tissues (macrophages, lung epithelia and intestine epithelia) and may reach 4% of total protein in the cytoplasm of human neutrophils (Perretti and D'Acquisto, 2009a).

In many inflammatory and cellular settings, the anti-inflammatory actions of ANXA1 are reproduced by peptides derived from the N-terminal region of the protein, including the peptide Ac2-26 (Perretti *et al.*, 1993; Perretti and Dalli, 2009b). This peptide, as well as the whole protein, exerts its effects through activation of the formyl peptide receptor type 1 (FPR1) and type 2 (FPR2) (Walther *et al.*, 2000a; Ernst *et al.*, 2004). Besides the effect on leukocyte migration, ANXA1 and its mimetics promote inhibition of epithelial cell proliferation (Croxtall *et al.*, 1993; 1998a), induction of phagocytosis of immune complexes by macrophages and apoptosis of inflammatory cells (Maderna *et al.*, 2005; Scannell *et al.*, 2007).

In this study we investigated the effect of the ANXA1 mimetic peptide Ac2-26 on the lung inflammatory response induced by silica particles. It was found to prevent the alterations in the lung function of silicotic mice, as well as reducing granuloma formation and collagen accumulation in the lung parenchyma. To verify the effect of Ac2-26 on the cellular response leading to fibrosis, we investigated the effect of this peptide on primary fibroblasts and showed that it reduced the production of collagen and CCL2 (MCP-1) by these cells, with no effect on proliferation, through a mechanism involving the FPR1.

Methods

Animals

Male Swiss-Webster, wild-type (WT) littermate (Balb/c) and ANXA1 knockout ($ANXA1^{-/-}$) mice (18–20 g) were obtained from the Oswaldo Cruz Foundation (Rio de Janeiro, Brazil) breeding unit and kept in the animal care facility of Oswaldo Cruz Institute. WT littermate (C57Bl6), $FPR1^{-/-}$ (Gao *et al.*,

1999) and FPR2$^{-/-}$ (Dufton *et al.*, 2010) were housed at the Biological Service Unit of Queen Mary University of London. In general, animals were maintained in ventilated cages (five mice per cage) under specific pathogen-free conditions in a room at 20–24°C, and relative humidity (40–70%) on a 12 h light/dark cycle with water and food *ad libitum*. This study was carried out in strict accordance with recommendations of the Animal Ethics Committee of the Oswaldo Cruz Foundation (licence L-034/09) and with the guidelines of the Ethical Committee for the Use of Animals, Barts and the London School of Medicine and Home Office Regulations (Guidance on the Operation of Animals, Scientific Procedures Act, 1986). In total 147 mice ($n = 7$ each group) were included in this study, and all efforts were made to minimize suffering. All animal experiments were conducted in accordance with Guide for the Care and Use of Laboratory Animals of the European council and were reported in accordance with the ARRIVE guidelines (Kilkenny *et al.*, 2010; McGrath *et al.*, 2010).

Silicosis induction and treatment

Silicosis was induced in halothane (Tanohalo, Cristália, São Paulo, Brazil) anaesthetized mice. Animals were then instilled intranasally with silica particles (10 mg 50 μL^{-1}; Sigma-Aldrich Corp., St Louis, MO, USA; 0.5–10 μM) and the control group received a similar volume of sterile saline (NaCl 0.9%) (Ferreira *et al.*, 2013). Analyses were performed 7 days post-silica instillation. The peptide Ac2-26 (Ac-AMVSEFLKQAWFIENEEQEYVQTVK) (200 μg per mouse; Cambridge Research Biochemicals, Cleveland, UK) and dexamethasone (25 μg per mouse; Sigma-Aldrich) were given intranasally for seven consecutive days, starting 6 h after silica provocation. Analyses were performed 24 h after the last administration.

Respiratory mechanics

Airway reactivity was assessed as a change in airway function after challenge with aerosolized methacholine in a Finepointe R/C Buxco® Platform (Buxco Research System, Willmington, NC, USA). Mice were anaesthetized with pentobarbital (60 $mg \cdot kg^{-1}$), and the neuromuscular activity was blocked with bromide pancuronium (1 $mg \cdot kg^{-1}$). The method used to assess the depth of anaesthesia was when the animal no longer reacted to a toe pinch. Tracheostomized animals were mechanically ventilated and lung function was assessed. The trachea was cannulated and the cannula connected to a pneumotachograph. Airflow and transpulmonary pressure were recorded with a Buxco lung resistance ($cmH_2O \cdot s \cdot mL^{-1}$) and dynamic lung compliance ($mL \cdot cmH_2O^{-1}$) in each breath cycle. Elastance was calculated as the inverse of compliance values. All signals were analogue-to-digital converted (Buxco analogical/digital converter). Animals were allowed to stabilize for 5 min, and increasing concentrations of methacholine (3–27 $mg \cdot mL^{-1}$) were aerosolized for 5 min each. Baseline pulmonary parameters were assessed with aerosolized PBS.

Histological analyses

The left lung was fixed in Milloning buffer solution (pH = 7.4) with 4% paraformaldehyde for 48 h to preserve tissue architecture. Samples were dehydrated in increasing concentrations of ethanol, clarified in xylene and then embedded in paraffin. Histological sections of 4 μm thick were made and stained with haematoxylin-eosin and Picrosirius. Lung morphometric analysis was performed by an integrating eyepiece with a coherent system consisting of a grid with 100 points and 50 lines (known length) (Gundersen *et al.*, 1988) coupled to a light microscope (Olympus BX50, Olympus America Inc., Center Valley, PA, USA) connected to a video camera (Optronics Engineering, DEI-750). The camera output was processed and examined by image analyser software Image-Pro Plus version 4 (Media-Cybernetics, Rockyville, MD, USA).

Immunohistochemistry

Expression of α-smooth muscle actin (α-SMA) in fibroblasts was determined by immunohistochemistry. After deparaffinization of histological sections, the material was rehydrated with TBS (Tris/HCl + 0.05 M NaCl 0.5 M, pH 7.6) and blocked with Tris-HCl + 5% BSA for 1 h. Then, monoclonal mouse antibody α-SMA (1:400; Tris-HCl + 1% BSA; Sigma, USA) was added and kept at 4°C overnight. The slides were washed twice with TBS or goat anti-mouse IgG (R&D Systems, Minneapolis, MN, USA) antibody conjugated to HRP was then added (both 1:80 in Tris-HCl) for 2 h. The 3-amino-9-ethylcarbazole was added for 15 min and the sections were counterstained with haematoxylin and analysed by light microscopy (Olympus BX51, Olympus America Inc.). In negative controls, primary antibody was omitted and tissues were incubated with antibody diluent only.

Collagen quantification

Right lungs were homogenized with Tris-NaCl (0.05:1 M) containing a protease inhibitor mix (Sigma), and total soluble collagen was extracted overnight at room temperature. Quantification of collagen was made using the Sircol™ kit (Biocolor Ltd., Newtonabbey, UK). The results are expressed as mg collagen per right lung.

ELISA analysis

Right lungs from saline- and silica-exposed mice were homogenized in 0.1% Triton X-100 solution containing a protease inhibitor mix (Sigma). After centrifugation (13 000× *g*, 10 min at 4°C), an aliquot was used to quantify CXCL1 (KC), CXCL2 (MCP-2), CCL2 (MCP-1), TNF-α, TGF-β and IFN-γ. Reagents from a commercial DuoSet Kit (R&D Systems) were used following the instructions of the manufacturer.

Lung fibroblast isolation and activation

FPR1$^{-/-}$, FPR2$^{-/-}$ and WT littermate mice were killed with CO_2. The lungs were perfused under aseptic conditions and subjected to enzymatic digestion by collagenase I at 37°C for 2 h. Cells were maintained in DMEM containing 20% FBS, 1% penicillin-streptomycin at 37°C and at 5% CO_2 and used until passage 7, when the phenotype was maintained (not shown). Then, 25×10^4 cells were added to 6-well plates and incubated with peptide Ac2-26 (5–30 μM) at 37°C and a 5% CO_2 for 24 h. The cells were stimulated with IL-13 (40 $ng \cdot mL^{-1}$) and TGF-β (10 $ng \cdot mL^{-1}$) for 24 h, and after centrifugation the supernatant was collected for collagen and CCL2 (MCP-1) quantification by Sircol and ELISA respectively.

Real-time PCR

RNA was isolated from 2.5 × 10^5 WT lung fibroblasts using TRIzol reagent (Invitrogen Life Technologies, São Paulo, Brazil). Contaminating genomic DNA was removed using DNase I (Turbo DNAse treatment, Ambion, Applied Biosystems, Foster City, CA, USA). The RNA was reverse-transcribed using oligo-dT (50 μM; Invitrogen) and dNTP (10 mM; Bioline, London, UK) at 65°C for 5 min, then in ice for 1 min. The RNA was incubated with Mastermix solution (first-strand buffer 5× – Invitrogen; DTT 0.1 M – Invitrogen; RNAse out and SuperScript III – Invitrogen) at 50°C for 15 min and then at 70°C for 15 min. The synthesized cDNA was used for real-time PCR. The cDNA was amplified by real-time PCR using primers specific for the receptors FPR1 and FPR2. FPR1, forward (5′-CAGAATTCCAGCCATGGACACCAACATGTCTC-3′) and reverse (5′-GCGAATTCTTTACATTGCATTTAAAGTG-3′); and for FPR2, forward (5′-GTCAAGATCAACAGAAGAA ACC-3′) and reverse (5′-GGGCTCTCTCAAGACTATAAGG-3′). The PCR reaction was performed at 94°C for 2 min and 30 s followed by 30 cycles of 94°C for 30 s, 58°C for 60 s and 72°C for 60 s with a final extension of 72°C for 15 min. The mRNA expression for both receptor subtypes was calculated and normalized according to mRNA expression of α-actin. In another set of experiments, lung fibroblasts were stimulated with IL-13 (40 ng·mL^{-1}) and TGF-β (10 ng·mL^{-1}) for 24 h, and then evaluated for the expression of FPR mRNA.

Statistical analysis

Results are expressed as mean ± SEM and statistical analysis was performed with one-way ANOVA followed by the multiple comparison test of Newman–Keuls–Student. Experimental number *n* was determined and validated by power analysis; as an example, for lung fibroblasts experiments, a three-way ANOVA was conducted (cytokine treatment, peptide application, genotype) justifying the *n* number used with a power of 80% for moderate-to-large effect size (η^2 = 0.15). Values of $P < 0.05$ were considered statistically significant for both tests.

Results

A lack of ANXA1 exacerbates inflammatory and fibrotic responses and alters lung function of silica-exposed mice

Levels of cytokines such as CXCL1 (KC), CXCL2 (MIP-2) and CCL2 (MCP-1) as well as TNF-α, IFN-γ and TGF-β were increased in the lung tissue of silicotic mice compared with saline-stimulated group. ANXA1$^{-/-}$ mice exposed to silica clearly showed even higher levels of these pro-inflammatory mediators in comparison with their WT littermate controls, with the exception of CCL2 (MCP-1) (Table 1).

Instillation of saline to WT and ANXA1$^{-/-}$ mice did not lead to abnormal deposition of collagen (Figure 1A,B respectively). In contrast, WT mice administered silica showed a massive increase in extracellular matrix deposition as revealed by the Picrosirius staining (Figure 1C). These changes were also noted in ANXA1$^{-/-}$ mice, but an increase in Picrosirius staining was observed in this group (Figure 1D). These histological results were confirmed by measuring total collagen content in the lung tissue (Figure 1E). Both WT and ANXA1$^{-/-}$ silica-stimulated mice had significantly higher levels of collagen than corresponding animals treated with saline (Figure 1E). Moreover, there was a statistically significant difference between WT and ANXA1$^{-/-}$ silica-stimulated mice, showing a higher degree of pulmonary fibrosis in the latter (Figure 1E). A marked granulomatous response in the lung parenchyma of WT and ANXA1$^{-/-}$ mice was also observed 7 days post-silica, but no significant difference in the granulomatous area was detected between these two groups (data not shown).

Lung resistance and elastance in anaesthetized and tracheostomized mice were evaluated to assess putative changes in airway function following administration of silica under conditions of deletion of ANXA1. As shown in Figure 1F, WT and ANXA1$^{-/-}$ silicotic mice reacted with comparable elevations in the baseline levels of airway resistance as compared with their corresponding saline-exposed group. In contrast,

Table 1

Role of endogenous ANXA1 in the production of cytokines in the lung tissue of saline- and silica-challenged mice

	ANXA1$^{+/+}$		ANXA1$^{-/-}$	
Cytokines	**Saline (ρg per right lung)**	**Silica (ρg per right lung)**	**Saline (ρg per right lung)**	**Silica (ρg per right lung)**
CXCL1 (KC)	927.2 ± 86.2	2304.1 ± 341.2*	1214.7 ± 98.1	3578.58 ± 385.0*$^+$
CCL2 (MCP-1)	302.0 ± 71.3	1522.2 ± 57.7*	339.4 ± 40.3	1703.89 ± 155.0*
CXCL2 (MIP-2α)	280.3 ± 93.6	531.4 ± 113.4*	293.0 ± 43.8	852.18 ± 69.7*$^+$
TNF-α	103.2 ± 6.8	136.8 ± 15.6*	126.8 ± 15.2	192.69 ± 23.9*$^+$
TGF-β	201.1 ± 18.9	266.0 ± 12.3	232.2 ± 12.9	258.92 ± 17.1
INF-γ	40.8 ± 6.2	69.2 ± 13.7*	46.6 ± 11.1	106.17 ± 4.7*$^+$

The analyses were performed 7 days after intranasal instillation of silica in WT (ANXA1$^{+/+}$) and knockout (ANXA1$^{-/-}$) mice. The values represent the mean ± SEM from six to eight animals. *$P < 0.05$ compared with the respective saline-challenged control group; $^+P < 0.05$ compared with ANXA1$^{+/+}$silica-challenged group.

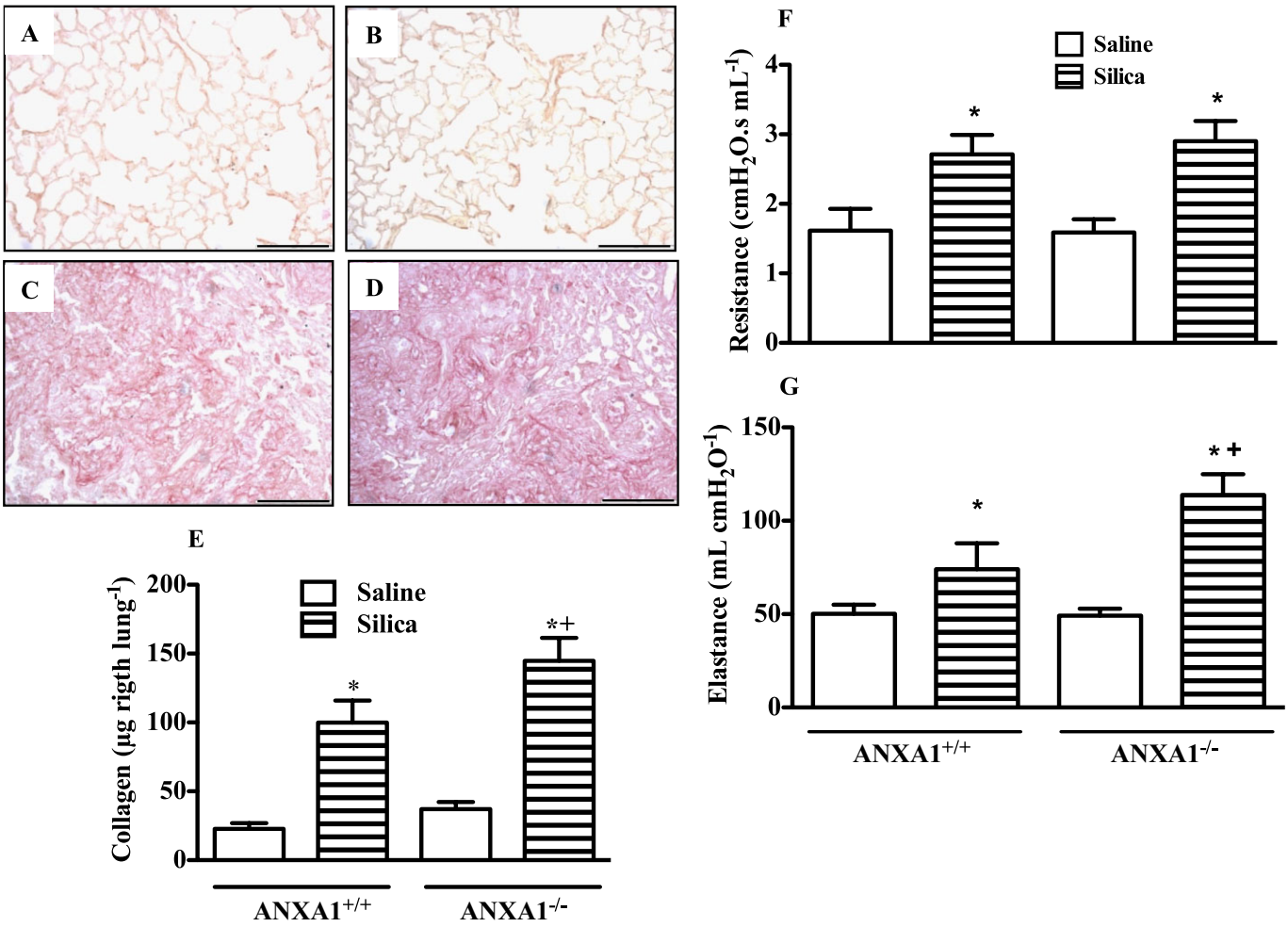

Figure 1

Analysis of endogenous ANXA1 during silica-induced lung fibrosis in WT (ANXA1$^{+/+}$) and ANXA1 knockout (ANXA1$^{-/-}$) mice. (A–D) Picrosirius Red-stained sections of lung tissue after silica and saline challenge. (E) Quantification of total content of tissue collagen by the Sircol technique. (F) Basal levels of lung resistance and (G) elastance. All analyses were performed on day 7 after silica challenge (10 mg per animal). Scale bar = 200 µm. Values represent the mean ± SEM from seven animals. *$P < 0.05$ compared with the respective saline-challenged control group; $^{+}P < 0.05$ compared with ANXA1$^{+/+}$ silica-challenged group.

silica-stimulated ANXA1$^{-/-}$ mice showed higher levels of lung elastance when compared with the WT controls (Figure 1G).

Inhibitory effect of peptide Ac2-26 on lung function and airway hyper-reactivity in silica-exposed mice

Peptide Ac2-26 retains the majority of the anti-inflammatory properties of ANXA1; hence, it was used here to assess its potential in experimental silicosis in comparison with dexamethasone. Exposure of mice to silica particles yielded higher baseline lung resistance when compared with the saline group. After aerosolization of the bronchoconstrictor methacholine, silica-stimulated mice exhibited increased airway resistance (Figure 2A). Intranasal treatment with peptide Ac2-26 (200 µg per mouse), but not dexamethasone (25 µg mouse), inhibited silica-induced up-regulation of lung resistance levels noted after aerosolization of methacholine (Figure 2A). Airway hyper-reactivity to methacholine in silicotic mice was also observed with respect to lung elastance (Figure 2B). Again, peptide Ac2-26 was able to inhibit this response, whereas dexamethasone only had an inhibitory effect after the highest dose of methacholine (Figure 2B).

Histopathological analysis of lungs from silicotic mice treated with peptide Ac2-26

We then tested whether treatment of mice with an ANXA1 mimetic would affect the dramatic changes provoked by silica in the lung. The saline-exposed group showed lung parenchyma with normal morphology and alveolar architecture was well defined with no evidence of inflammation (Figure 3A). In contrast, an intense inflammatory infiltrate and formation of granuloma were observed after silica provocation (Figure 3B). Treatment with dexamethasone partially reduced the inflammatory infiltrate and granulomatous

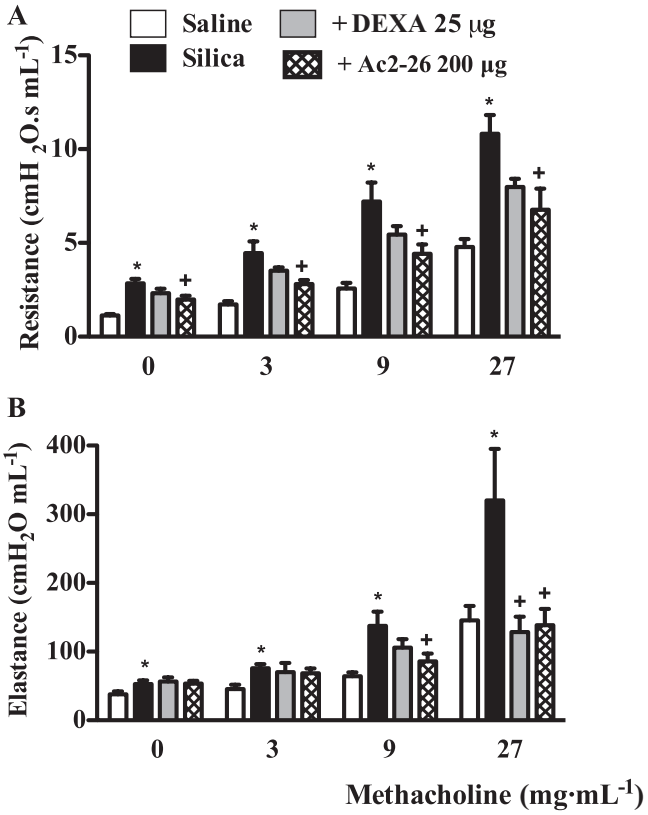

Figure 2

Airway hyper-reactivity measured as resistance (A) and elastance (B) induced by provocation with increasing concentrations of methacholine in mice challenged with silica (10 mg) and treated with dexamethasone (DEXA; 25 µg per mouse) or peptide Ac2-26 (200 µg per mouse). Animals instilled with saline were used as controls. The analyses were made on day 8 after silica challenge. Values represent mean ± SEM from seven animals. $^{+}P < 0.05$ as compared with saline-challenged group. $*P < 0.05$ as compared with silica-challenged group.

response (Figure 3C), which were also clearly sensitive to peptide Ac2-26 (200 µg per mouse) (Figure 3D). As shown in Figure 3E, the lung area occupied by silica-induced granuloma was significantly reduced following treatment with dexamethasone and peptide Ac2-26. The effectiveness of both treatments was confirmed by measuring collagen production in lung samples (Figure 3F).

Inhibitory effect of peptide Ac2-26 on production of inflammatory mediators in lungs from silica-exposed mice

The tissue-protective effect of peptide Ac2-26, evident both macroscopically and microscopically, was associated with a marked reduction in the tissue levels of CXCL1 (KC) (Figure 4A), CCL2 (MCP-1) (Figure 4B), TGF-β (Figure 4C) and TNF-α (Figure 4D), but not IFN-γ (Figure 4E). Dexamethasone slightly inhibited only the generation of CCL2 (MCP-1) (Figure 4B).

Expression α-SMA in lung parenchyma of silica-exposed mice is sensitive to peptide Ac2-26

Important plastic changes occur in fibrotic lungs with fibroblasts and their phenotype changes, with cells expressing α-SMA and becoming myofibroblasts. On analysis of lungs from the saline-exposed group, we found no labelling for myofibroblasts (Figure 5A). Silica-stimulated mice showed an intense fibrotic response, and the granulomatous area and adjacent regions were highly positive for α-SMA (Figure 5B). The labelling for α-SMA was clearly reduced following treatment with both dexamethasone (Figure 5C) and peptide Ac2-26 (Figure 5D).

Peptide Ac2-26 inhibits collagen and cytokine secretion of lung fibroblasts in vitro

Next we assessed the direct effect of peptide Ac2-26 on lung fibroblasts. These cells are important in the process of fibrosis as they were shown to produce extracellular matrix components and pro-fibrotic cytokines such as collagen and CCL2 (MCP-1) respectively. IL-13 (40 ng·mL^{-1}) and TGF-β (10 ng·mL^{-1}) induced a proliferative response of fibroblasts, which remained unaltered after treatment with peptide Ac2-26 (7.5–30 µM) (data not shown). In contrast, peptide Ac2-26 inhibited, in a concentration-dependent manner, both collagen and CCL2 (MCP-1) production triggered by IL-13 (Figure 6A,C) and TGF-β (Figure 6B,D). These findings indicate that peptide Ac2-26 failed to interfere with lung fibroblast proliferation, although it directly inhibited collagen and CCL2 (MCP-1) production.

Involvement of FPR1 and FPR2 in the suppressive effect of peptide Ac2-26 on lung fibroblast activation

The peptide Ac2-26 exerts its anti-inflammatory effects by binding to FPR1 and FPR2. Using real-time PCR, we demonstrated that mRNA for FPR1 and FPR2 is already expressed on lung fibroblasts. Under conditions of stimulation with IL-13 and TGF-β, a significant increase in FPR1 and FPR2 mRNA expression was noted in the case of IL-13 (40 ng·mL^{-1}) (Table 2). No alteration was detected after stimulation with TGF-β (10 ng·mL^{-1}) (Table 2).

Lung fibroblasts from WT and FPR1$^{-/-}$ mice produced higher levels of collagen and CCL2 (MCP-1) after stimulation with IL-13 (40 ng·mL^{-1}) and TGF-β (10 ng·mL^{-1}) as compared with non-stimulated cells (data not shown). However, cells from FPR1$^{-/-}$ mice when stimulated with IL-13 and TGF-β showed no response after incubation with peptide Ac2-26 (Figure 7B,D), while production of collagen and CCL2 (MCP-1) was inhibited in WT fibroblasts (Figure 7A,C). Lung fibroblasts from FPR2$^{-/-}$ mice showed similar responses to those of the WT cells, with regards to collagen and MCP-1 release after stimulation with IL-13 and TGF-β (data not shown). The peptide Ac2-26 did not affect collagen production by cells from WT and FPR2$^{-/-}$ mice (Figure 8A,B), whereas the production of CCL2 (MCP-1) was shown to be sensitive to the peptide (Figure 8C,D). These data suggest an important role for FPR1 in the suppressive effect of peptide Ac2-26 on

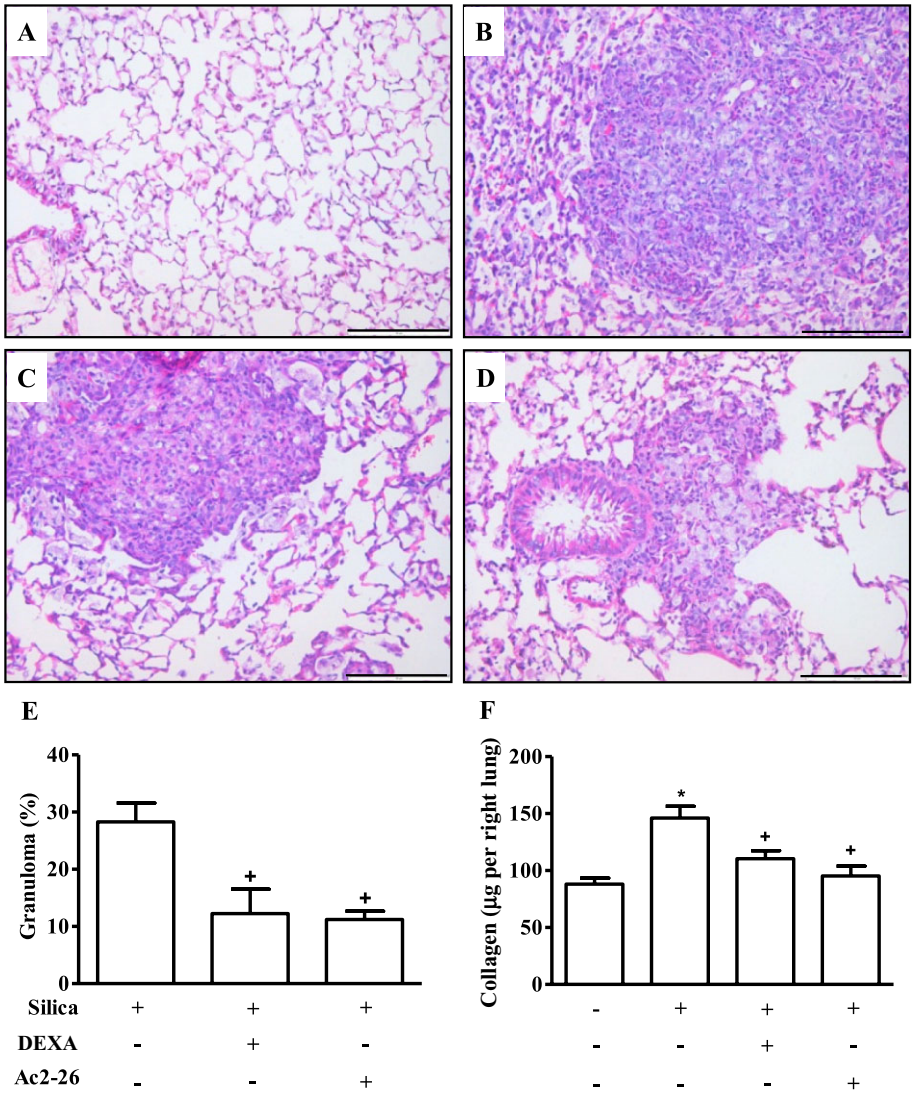

Figure 3

Histological sections of mouse lung on day 8 after saline (A) or silica challenge (B) and subsequently given intranasal treatment with dexamethasone (DEXA; 25 µg per mouse) (C) and peptide Ac2-26 (200 µg per mouse) (D). Morphometric analysis and total tissue collagen content are seen in panels E and F respectively. Slides were stained with haematoxylin-eosin. Scale bar = 200 µM. Values represent mean ± SEM from seven animals. *$P < 0.05$ as compared with saline-challenged group. $^{+}P < 0.05$ as compared with silica-challenged group.

collagen and CCL2 (MCP-1) production by lung fibroblasts, while the FPR2 seems to be important only for collagen production.

Discussion and conclusions

The present study reveals novel protective properties of ANXA1 on the inflammatory and fibrotic responses triggered by silica particles in the airways of mice. It also provides evidence that ANXA1 mimetic agents can be a promising therapeutic strategy as an innovative anti-fibrotic approach for the treatment of silicosis.

ANXA1 and some of its derivatives were shown to be effective in inhibiting cell proliferation, although there are still some controversies in the literature. Lung epithelial cells are down-regulated by ANXA1 and its mimetic Ac2-26 (Croxtall *et al.*, 1993, 1998b). On the other hand, Kurosu *et al.* (2008) reported that the N-terminal derivative of ANXA1 (peptide 18–26) induced a marked proliferative response of CD4-positive cells from 3 out of 15 patients showing acute exacerbation of idiopathic pulmonary fibrosis. It has been demonstrated that the constituents of ANXA1, required for FPR1 receptor activation, are shown to be within the 2–12 pharmacophore region of the molecule (Perretti *et al.*, 2001), which indicates that the length of the ANXA1

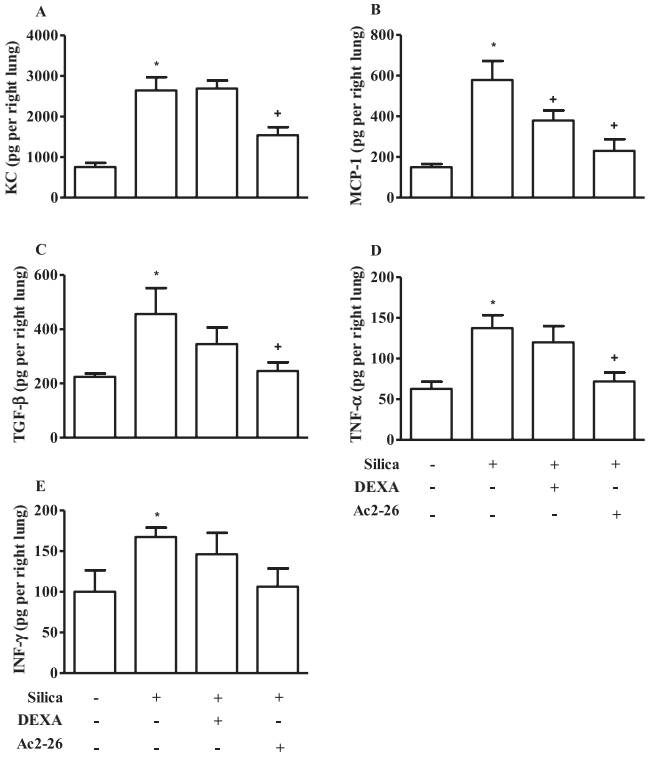

Figure 4

Production of (A) CXCL1 (KC), (B) CCL2 (MCP-1), (C) TGF-β, (D) TNF-α and (E) IFN-γ in lung samples of mice treated with dexamethasone (DEXA; 25 μg per mouse) and peptide Ac2-26 (200 μg per mouse) from 6 h to 7 days after silica challenge (10 mg). Animals instilled with saline were used as controls. The analyses were made on day 8 after silica challenge. Values represent mean ± SEM from seven animals. *$P < 0.05$ as compared with saline-challenged group. $^{+}P < 0.05$ as compared with silica-challenged group.

derivatives seems to be crucial for their biological effects. Differences in the experimental systems and target cells may also explain some of the discrepancies noted in the effect of ANXA1-derived peptides as emphasized in the literature. In the present study, we demonstrated a non-redundant function for mouse FPR1 as shown using the knockout mice and the peptide Ac2-26 that contains the putative pharmacophore region. Our data showed changes in parameters of respiratory mechanics of silicotic mice, expressed by increased lung resistance and elastance, followed by hyper-reactivity of airway after stimulation with the bronchoconstrictor cholinergic agent, methacholine. These results confirm previous findings from our group that revealed the occurrence of obstructive and restrictive changes in lungs of silicotic mice (Ferreira *et al.*, 2013). The airway hyper-reactivity verified is in agreement with findings in humans (Forastiere *et al.*, 2002; Montes *et al.*, 2004). It was shown that exposure to high concentrations of crystalline silica promotes an intense inflammatory response accompanied by cell proliferation and excessive deposition of collagen and other extracellular matrix components, resulting in the development of fibrosis (Mossman and Churg, 1998). Thus, changes in lung function of animals with silicosis are directly related to alterations in lung parenchyma, which in turn reflect the presence of an intense inflammatory infiltrate and granuloma formation.

In this study, ANXA1$^{-/-}$ mice reacted to silica exposure with a marked exacerbation of lung inflammation and remodelling changes as compared with WT mice. Such an exacerbation correlated well with elevated levels of pro-inflammatory cytokines in the lung tissue as well as with higher levels of elastance. Furthermore, the intranasal treatment of silicotic mice with the ANXA1 mimetic peptide Ac2-26 improved lung function and reversed granuloma formation, collagen deposition and cytokine production triggered by silica particles in this experimental model. In addition, we showed that peptide Ac2-26 had an important inhibitory effect on the reactivity of lung fibroblasts *in vitro*, and that FPR1 and FPR2 are involved in this response.

The improvement caused by peptide Ac2-26 in the lung parenchyma may have contributed to the restoration of lung function in silicotic animals. Peptide Ac2-26 is derived from the N-terminal region of ANXA1, which is associated with the anti-inflammatory activity of this protein. Some anti-inflammatory effects of glucocorticoids were shown to be mediated by ANXA1 (Parente and Perretti, 2003). In this way, treatment with the glucocorticoid dexamethasone was used as a control in the experiments conducted *in vivo*. Getting *et al.* (1997) demonstrated that dexamethasone inhibited the infiltration of neutrophils and monocytes in an acute inflammatory model, induced by zymosan, through a mechanism mediated by the ANXA1 protein. They also reported that peptide Ac2-26 markedly reduced the migration of neutrophils and monocytes to the injured site. Thus, it is believed that part of the inhibitory effect of dexamethasone in silicotic mice may be mediated by ANXA1. However, the glucocorticoid only partially affected the damage evoked by silica when compared with peptide Ac2-26.

In this study, the peptide Ac2-26 significantly reduced the production of cytokines CXCL1 (KC), CCL2 (MCP-1) and IFN-γ in the lungs of silicotic animals, which contributed to the reduction of the inflammatory response. In addition, our data are in agreement with reduced labelling for macrophages (F4/80) in lungs of mice treated with the peptide, indicating a decreased activation and migration of these cells to the injured site. The local treatment with dexamethasone did not interfere with the production of CXCL1 (KC) and only partially affected CCL2 (MCP-1) as well as leukocyte migration to the lung tissue. Furthermore, we demonstrated that the peptide Ac2-26 effectively inhibited both collagen deposition as well as labelling of α-SMA in lungs of silicotic mice. This phenomenon can be correlated to the inhibition of pro-fibrotic cytokine generation such as TGF-β and TNF-α. Previous studies showed that ANXA1 has a regulatory effect on the production of inflammatory cytokines such as TNF-α and IL-1β through inhibition of NF-κB activation (Sudlow *et al.*, 1996; D'Acquisto *et al.*, 1997). In line with this observation, ANXA1 and the derived peptide Ac2-26 were shown to suppress proliferation and activation of the human epithelial cell line A 549 (Croxtall *et al.*, 1998b).

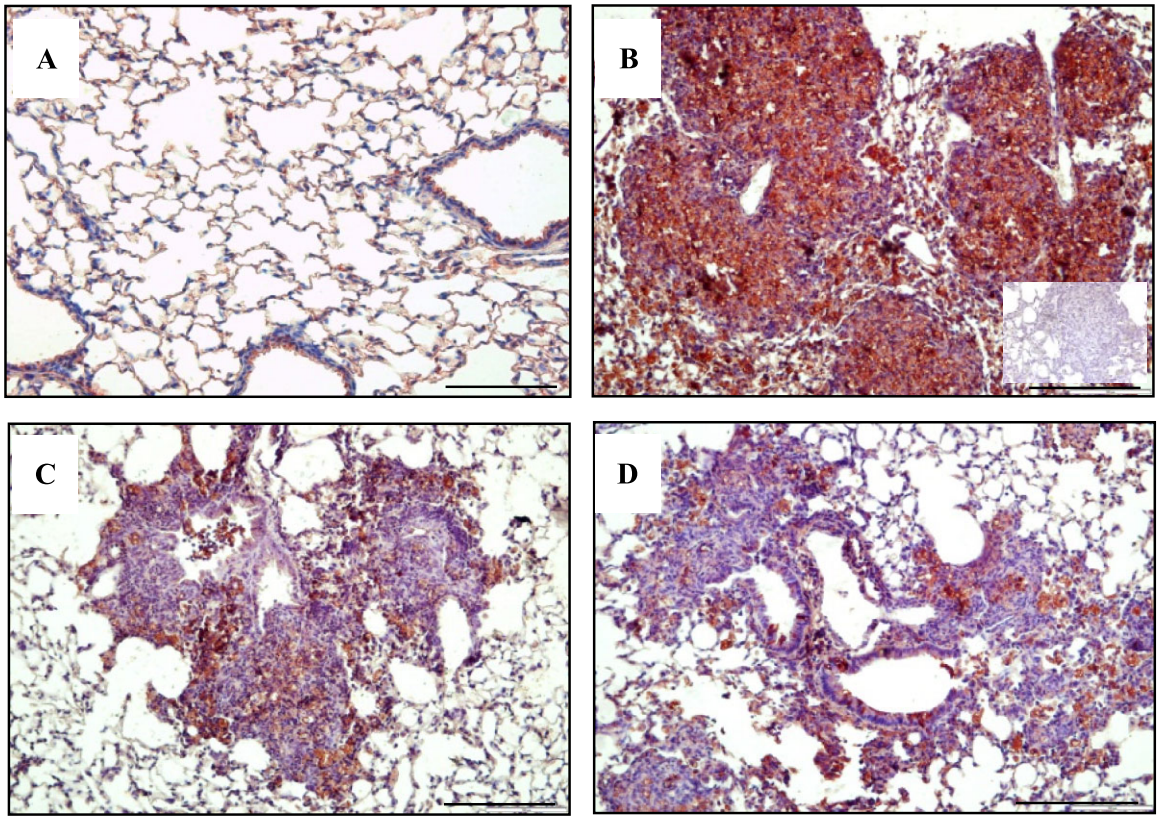

Figure 5

Immunohistochemical localization of α-SMA-positive cells in the lung sections of mice challenged with saline (A), silica (B), silica treated with dexamethasone (25 μg per mouse) (C) and silica treated with Ac2-26 peptide (200 μg per mouse) (D). Treatment was performed for seven consecutive days, starting 6 h post-silica challenge (10 mg). The analyses were made 1 day after the last administration, on day 8 after silica challenge. The inset shows negative control in which primary antibody was omitted. Scale bar = 200 μM.

Silica particles are able to stimulate directly lung fibroblasts (Arcangeli *et al.*, 2001; Baroni *et al.*, 2001), which are considered as a crucial source of extracellular matrix components (collagen) and pro-fibrotic cytokines (such as CCL2) (Galindo *et al.*, 2001; Hao *et al.*, 2003). As fibroblasts are important cells in the development of lung fibrosis triggered by particles of silica, we assessed the direct action of peptide Ac2-26 on these cells. Contrary to our expectations, treatment with the peptide did not alter the proliferation rate of fibroblasts when they were stimulated with IL-13 and TGF-β, but inhibited, in a concentration-dependent manner, the production of collagen and CCL2 (MCP-1). These results are in line with data obtained from *in vivo* experiments, which showed a reduction of both collagen and CCL2 (MCP-1) in the lung tissue. These findings suggest that the peptide Ac2-26 exerts a suppressive effect on lung fibroblast activation, but not on proliferation, leading to inhibition of the generation of inflammatory mediators and extracellular matrix components. Thus, in this way, the peptide can reduce the fibrosis induced by silica.

ANXA1 and peptide Ac2-26 exert their inhibitory effect on leukocyte migration through an interaction with the GPCRs, belonging to the family of FPR (Walther *et al.*, 2000b; Hayhoe *et al.*, 2006), which are present on the cellular membrane of leukocytes (Perretti *et al.*, 2002). Glucocorticoids induce the expression of ANXA1 and FPRs on monocytes and polymorphonuclear leukocytes (Goulding *et al.*, 1990; Damazo *et al.*, 2006; Sawmynaden and Perretti, 2006). As the peptide Ac2-26 had a marked inhibitory effect on the production of collagen and CCL2 (MCP-1) by lung fibroblasts *in vitro*, we assessed the involvement of FPR1 and FPR2 receptors in this response. For the first time, the mRNA expression for both types of FPR was detected in lung fibroblast under basal conditions. Moreover, an increase in the mRNA expression for FPR1 and FPR2 receptors was detected after stimulation with IL-13. Further investigations are needed to clarify this response.

Using lung fibroblasts from mice with deleted FPR1 or FPR2, we assessed the production of collagen and CCL2 (MCP-1) by these cells after stimulation with IL-13 or TGF-β. Our data revealed that cells from $FPR1^{-/-}$ mice when treated with peptide Ac2-26 showed no reduction in collagen and CCL2 (MCP-1) production, a response different from that noted with WT cells. In contrast, the peptide inhibited the production of CCL2 (MCP-1) by fibroblasts from $FPR2^{-/-}$ mice, although it did not affect the production of collagen in these fibroblasts. These results indicate that FPR1 and FPR2 mediate inhibition of lung fibroblast

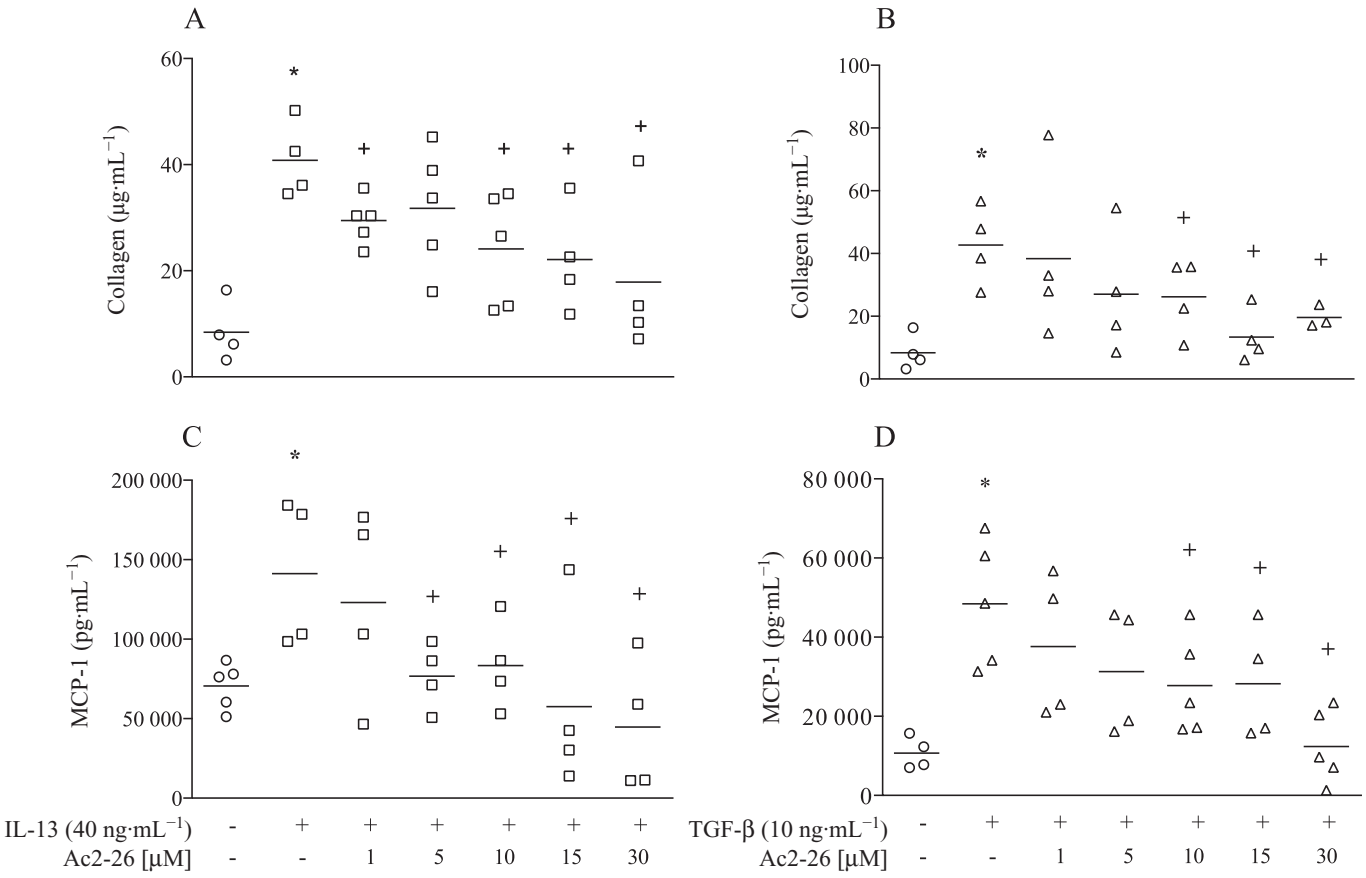

Figure 6

Activation of cultured lung fibroblasts recovered from ANXA1 WT (ANXA1$^{+/+}$) mice. Production of collagen (upper panels) and CCL2 (MCP-1) (lower panels) after stimulation with IL-13 (40 ng·mL^{-1}) (A, C) and TGF-β (10 ng·mL^{-1}) (B, D). Cells were exposed to peptide Ac2-26 (1–30 µM) 1 h before stimulation, and the analyses performed in the supernatant 24 h later. Values represent data from four to five independent experiments. Means were significantly different as analysed by ANOVA. (A) *F*-value = 4.59 ($P < 0.0031$); (B) *F*-value = 2.65 ($P = 0.0468$); (C) *F*-value = 3.4 ($P < 0.00025$) and (D) *F*-value = 4.45 ($P < 0.0037$).

Table 2

mRNA expression of FPR1 and FPR2 on lung fibroblasts recovered from WT (C57Bl6) mice

	ΔΔCt (real-time PCR)	
Stimulus	**FPR1**	**FPR2**
Medium	25.79 ± 0.04	28.53 ± 0.23
IL-13	27.75 ± 0.10*	30.98 ± 0.34*
TGF-β	25.98 ± 0.04	29.14 ± 0.25

Cells were stimulated with IL-13 (40 ng·mL^{-1}) and TGF-β (10 ng·mL^{-1}) for 24 h. Values are presented as mean ± SEM of triplicates. $n = 4$. *$P < 0.05$ compared with the respective non-stimulated control group.

activation by peptide Ac2-26. However, only FPR1 seems to mediate the peptide's inhibitory effect on the production CCL2 (MCP-1). This clearly indicates that peptide Ac2-26 acts by different mechanisms to down-regulate lung fibroblast activation.

Taken together, our findings show that peptide Ac2-26 acts on FPR1 and FPR2 leading to a reduction in fibrotic and chemotactic cytokines, which results in inhibition of leukocyte migration and collagen deposition in the lung parenchyma. Thus, the improvement in fibrosis and inflammation leads to a restoration of lung function in silicotic mice, indicating a pharmacological association that could possibly lead to the development of a therapeutic agent for silicosis.

Acknowledgements

We thank Rodrigo Azevedo and Nathália de Andrade Guimarães for skilful technical assistance and also Mr HR Jones

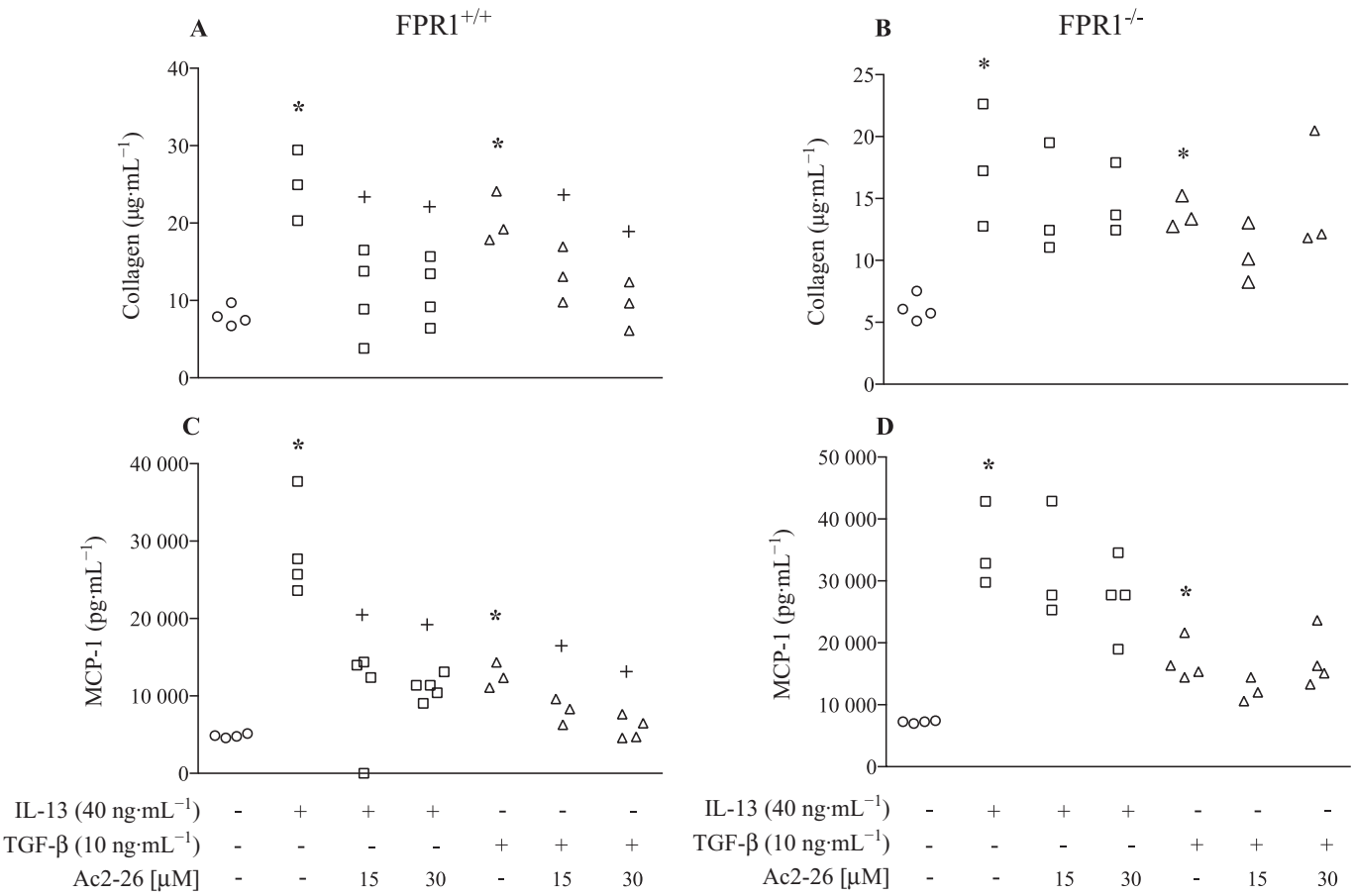

Figure 7

Activation of cultured lung fibroblasts recovered from FPR1 WT (FPR1$^{+/+}$) (A, C) and knockout (FPR1$^{-/-}$) mice (B, D). Production of collagen (upper panels) and CCL2 (MCP-1) (lower panels) after stimulation with IL-13 (40 ng·mL^{-1}) and TGF-β (10 ng·mL^{-1}). Cells were exposed to peptide Ac2-26 (15 and 30 µM) 1 h before stimulation and the analyses performed in the supernatant 24 h later. Values represent data from three to four independent experiments. Means were significantly different as analysed by ANOVA . (A) *F*-value = 8.27 ($P < 0.0003$); (B) *F*-value = 4.27 ($P = 0.011$); (C) *F*-value = 18.00 ($P < 0.0001$) and (D) *F*-value = 13.36 ($P < 0.0001$).

(William Harvey Research Institute) for statistical support. The research leading to these results has received funding from Conselho Nacional de Desenvolvimento Científico e Tecnológico (CNPq- 476470/2009-9), Fundação Carlos Chagas de Apoio à Pesquisa do Estado do Rio de Janeiro (FAPERJ- E-26/110.314/2010; E-26/102.853/2012) and the European Community's Seventh Framework Programme (FP7-2007-2013) under grant agreement n HEALTH-F4-2011-281608. This work was also supported by fellowships – Research Productivity Fellowship to P. M. R. S., M. A. M. and R. S. B. C. from CNPq; post-doc to T. P. T. F. and B. T. C. from CNPq/FIOCRUZ and P. G. T. from FAPERJ/CAPES.

Author contributions

P. G. T. was responsible for acquisition, analysis and interpretation of data for this work and provided illustration. T. P. T. F. was responsible for acquisition and analysis of data for this work and provided illustration. A. C. S. A. and B. T. C. were responsible for acquisition and analysis of data for this work. R. S. B. C. drafted this work and contributed to financing. R. J. F. critically revised the manuscript for important intellectual content. M. P. was responsible for the analysis of data for this work, and contributed to manuscript writing and revision. M. A. M. made substantial contributions to the design of this work, revised it critically for important intellectual content and financing. P. M. R. S. was responsible for the design of this work, supervision, final approval and financing. Agreement to be accountable for all aspects of this work in ensuring that questions related to the accuracy or integrity of any part of the work are appropriately investigated and resolved.

Conflict of interest

None.

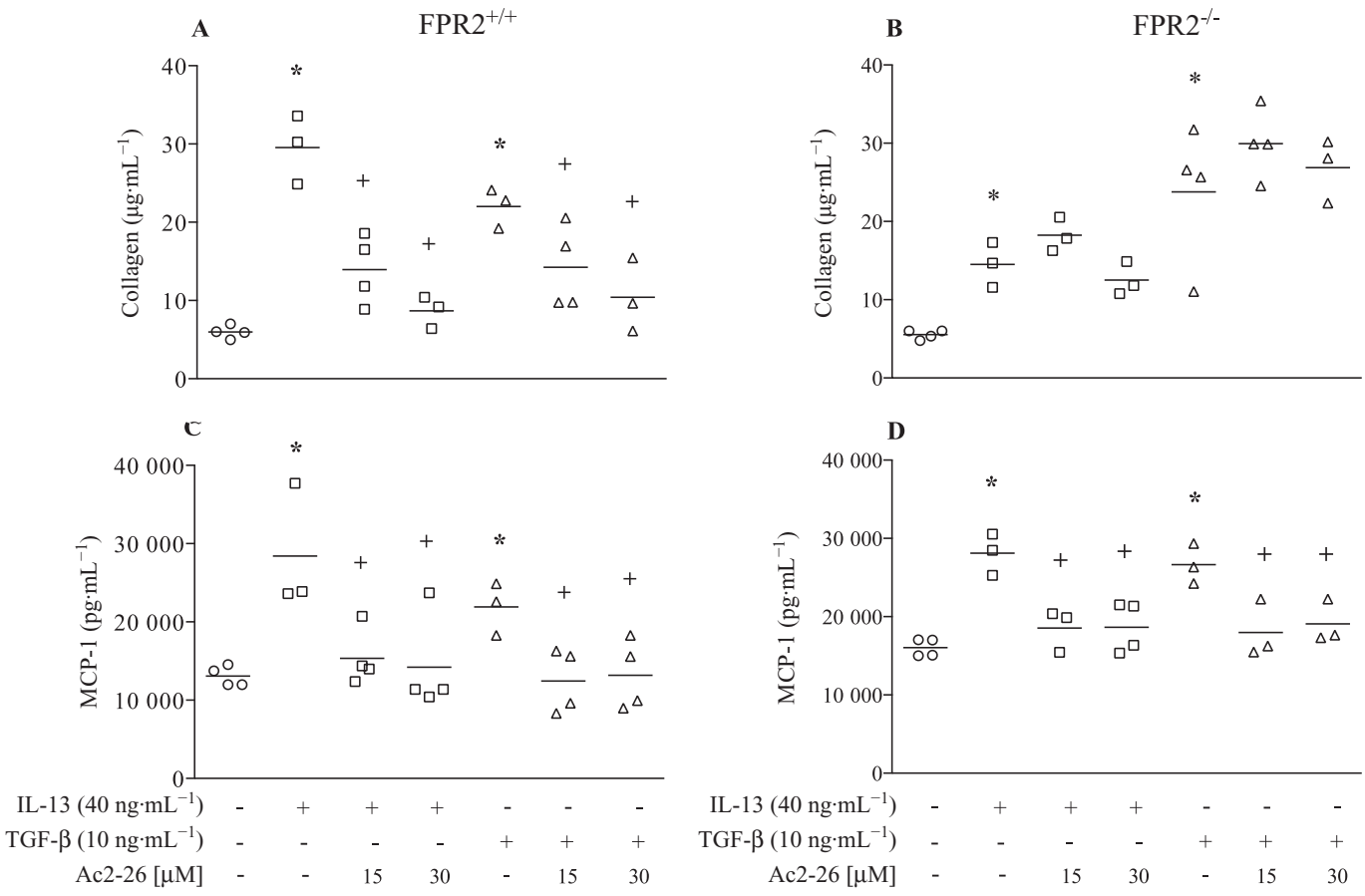

Figure 8

Activation of cultured lung fibroblasts recovered from FPR2 WT (FPR2$^{+/+}$) (A, C) and knockout (FPR2$^{-/-}$) mice (B, D). Production of collagen (upper panels) and CCL2 (MCP-1) (lower panels) after stimulation with IL-13 (40 ng·mL^{-1}) and TGF-β (10 ng·mL^{-1}). Cells were exposed to peptide Ac2-26 (15 and 30 µM) 1 h before stimulation, and the analyses performed in the supernatant 24 h later. Values represent data from three to four independent experiments. Means were significantly different as analysed by ANOVA. (A) *F*-value = 14.57 ($P < 0.0001$); (B) *F*-value = 12.95 ($P = 0.0001$); (C) *F*-value = 5.14 ($P < 0.0027$) and (D) *F*-value = 9.22 ($P < 0.0002$).

References

Alexander SPH, Benson HE, Faccenda E, Pawson AJ, Sharman JL, Spedding M *et al.* (2013). The Concise Guide to PHARMACOLOGY 2013/14: G protein-coupled receptors. Br J Pharmacol 170: 1459–1581.

Arcangeli G, Cupelli V, Giuliano G (2001). Effects of silica on human lung fibroblast in culture. Sci Total Environ 270: 135–139.

Baroni T, Bodo M, D'Alessandro A, Conte C, Calvitti M, Muzi G *et al.* (2001). Silica and its antagonistic effects on transforming growth factor-beta in lung fibroblast extracellular matrix production. J Investig Med 49: 146–156.

Carneiro AP, Barreto SM, Siqueira AL, Cavariani F, Forastiere F (2006). Continued exposure to silica after diagnosis of silicosis in Brazilian gold miners. Am J Ind Med 49: 811–818.

Croxtall JD, Waheed S, Choudhury Q, Anand R, Flower RJ (1993). N-terminal peptide fragments of lipocortin-1 inhibit A549 cell growth and block EGF-induced stimulation of proliferation. Int J Cancer 54: 153–158.

Croxtall JD, Choudhury Q, Flower RJ (1998a). Inhibitory effect of peptides derived from the N-terminus of lipocortin 1 on arachidonic acid release and proliferation in the A549 cell line: identification of E-Q-E-Y-V as a crucial component. Br J Pharmacol 123: 975–983.

Croxtall JD, Wu HL, Yang HY, Smith B, Sutton C, Chang BI *et al.* (1998b). Lipocortin 1 co-associates with cytokeratins 8 and 18 in A549 cells via the N-terminal domain. Biochim Biophys Acta 1401: 39–51.

Damazo AS, Yona S, Flower RJ, Perretti M, Oliani SM (2006). Spatial and temporal profiles for anti-inflammatory gene expression in leukocytes during a resolving model of peritonitis. J Immunol 176: 4410–4418.

Davis GS (1986). The pathogenesis of silicosis. State of the art. Chest 89 (3 Suppl.): 166S–169S.

D'Acquisto F, Cicatiello L, Iuvone T, Ialenti A, Ianaro A, Esumi H *et al.* (1997). Inhibition of inducible nitric oxide synthase gene expression by glucocorticoid-induced protein(s) in lipopolysaccharide-stimulated J774 cells. Eur J Pharmacol 339: 87–95.

Dufton N, Hannon R, Brancaleone V, Dalli J, Patel HB, Gray M *et al*. (2010). Anti-inflammatory role of the murine formyl-peptide receptor 2: ligand-specific effects on leukocyte responses and experimental inflammation. J Immunol 184: 2611–2619.

Ernst S, Lange C, Wilbers A, Goebeler V, Gerke V, Rescher U (2004). An annexin 1 N-terminal peptide activates leukocytes by triggering different members of the formyl peptide receptor family. J Immunol 172: 7669–7676.

Ferreira TP, de Arantes AC, do Nascimento CV, Olsen PC, Trentin PG, Rocco PR *et al*. (2013). IL-13 immunotoxin accelerates resolution of lung pathological changes triggered by silica particles in mice. J Immunol 191: 5220–5229.

Forastiere F, Goldsmith DF, Sperati A, Rapiti E, Miceli M, Cavariani F *et al*. (2002). Silicosis and lung function decrements among female ceramic workers in Italy. Am J Epidemiol 156: 851–856.

Fubini B, Hubbard A (2003). Reactive oxygen species (ROS) and reactive nitrogen species (RNS) generation by silica in inflammation and fibrosis. Free Radic Biol Med 34: 1507–1516.

Galindo M, Santiago B, Alcami J, Rivero M, Martin-Serrano J, Pablos JL (2001). Hypoxia induces expression of the chemokines monocyte chemoattractant protein-1 (MCP-1) and IL-8 in human dermal fibroblasts. Clin Exp Immunol 123: 36–41.

Gao JL, Lee EJ, Murphy PM (1999). Impaired antibacterial host defense in mice lacking the N-formylpeptide receptor. J Exp Med 189: 657–662.

Gerke V, Creutz CE, Moss SE (2005). Annexins: linking Ca2+ signalling to membrane dynamics. Nat Rev Mol Cell Biol 6: 449–461.

Getting SJ, Flower RJ, Perretti M (1997). Inhibition of neutrophil and monocyte recruitment by endogenous and exogenous lipocortin 1. Br J Pharmacol 120: 1075–1082.

Gettings SD, Lordo RA, Feder PI, Hintze KL (1998). A comparison of low volume, Draize and in vitro eye irritation test data. III. Surfactant-based formulations. Food Chem Toxicol 36: 209–231.

Gilroy DW, Lawrence T, Perretti M, Rossi AG (2004). Inflammatory resolution: new opportunities for drug discovery. Nat Rev Drug Discov 3: 401–416.

Goulding NJ, Godolphin JL, Sharland PR, Peers SH, Sampson M, Maddison PJ *et al*. (1990). Anti-inflammatory lipocortin 1 production by peripheral blood leucocytes in response to hydrocortisone. Lancet 335: 1416–1418.

Gundersen HJ, Bendtsen TF, Korbo L, Marcussen N, Moller A, Nielsen K *et al*. (1988). Some new, simple and efficient stereological methods and their use in pathological research and diagnosis. Acta Pathol Microbiol Immunol Scand 96: 379–394.

Hao L, Okada H, Kanno Y, Inoue T, Kobayashi T, Watanabe Y *et al*. (2003). Direct contact between human peripheral blood mononuclear cells and renal fibroblasts facilitates the expression of monocyte chemoattractant protein-1. Am J Nephrol 23: 208–213.

Hayhoe RP, Kamal AM, Solito E, Flower RJ, Cooper D, Perretti M (2006). Annexin 1 and its bioactive peptide inhibit neutrophil-endothelium interactions under flow: indication of distinct receptor involvement. Blood 107: 2123–2130.

Huaux F (2007). New developments in the understanding of immunology in silicosis. Curr Opin Allergy Clin Immunol 7: 168–173.

Kamal AM, Flower RJ, Perretti M (2005). An overview of the effects of annexin 1 on cells involved in the inflammatory process. Mem Inst Oswaldo Cruz 100 (Suppl. 1): 39–47.

Kilkenny C, Browne W, Cuthill IC, Emerson M, Altman DG (2010). Animal research: reporting *in vivo* experiments: the ARRIVE guidelines. Br J Pharmacol 160: 1577–1579.

Kurosu K, Takiguchi Y, Okada O, Sakao S, Kasahara Y, Tanabe N *et al*. (2008). Identification of annexin1 as a novel autoantigen in acute idiopathic pulmonary fibrosis. J Immunol 181: 756–767.

Leung CC, Yu IT, Chen W (2012). Silicosis. Lancet 379: 2008–2018.

Maderna P, Yona S, Perretti M, Godson C (2005). Modulation of phagocytosis of apoptotic neutrophils by supernatant from dexamethasone-treated macrophages and annexin-derived peptide Ac(2–26). J Immunol 174: 3727–3733.

Mariani TJ, Roby JD, Mecham RP, Parks WC, Crouch E, Pierce RA (1996). Localization of type I procollagen gene expression in silica-induced granulomatous lung disease and implication of transforming growth factor-beta as a mediator of fibrosis. Am J Pathol 148: 151–164.

McGrath JC, Drummond GB, McLachlan EM, Kilkenny C, Wainwright CL (2010). Guidelines for reporting experiments involving animals: the ARRIVE guidelines. Br J Pharmacol 160: 1573–1576.

Montes II, Rego G, Camblor C, Quero A, Gonzalez A, Rodriguez C (2004). Respiratory disease in aggregate quarry workers related to risk factors and Pi phenotype. J Occup Environ Med 46: 1150–1157.

Mossman BT, Churg A (1998). Mechanisms in the pathogenesis of asbestosis and silicosis. Am J Respir Crit Care Med 157 (5 Pt 1): 1666–1680.

Parente L, Perretti M (2003). Advances in the pathophysiology of constitutive and inducible cyclooxygenases: two enzymes in the spotlight. Biochem Pharmacol 65: 153–159.

Pawson AJ, Sharman JL, Benson HE, Faccenda E, Alexander SP, Buneman OP *et al*.; NC-IUPHAR (2014). The IUPHAR/BPS Guide to PHARMACOLOGY: an expert-driven knowledgebase of drug targets and their ligands. Nucl Acids Res 42 (Database Issue): D1098–D106.

Perretti M, Ahluwalia A, Harris JG, Goulding NJ, Flower RJ (1993). Lipocortin-1 fragments inhibit neutrophil accumulation and neutrophil-dependent edema in the mouse. A qualitative comparison with an anti-CD11b monoclonal antibody. J Immunol 151: 4306–4314.

Perretti M, Chiang N, La M, Fierro IM, Marullo S, Getting SJ *et al*. (2002). Endogenous lipid- and peptide-derived anti-inflammatory pathways generated with glucocorticoid and aspirin treatment activate the lipoxin A4 receptor. Nat Med 8: 1296–1302.

Perretti M, D'Acquisto F (2009a). Annexin A1 and glucocorticoids as effectors of the resolution of inflammation. Nat Rev Immunol 9: 62–70.

Perretti M, Dalli J (2009b). Exploiting the Annexin A1 pathway for the development of novel anti-inflammatory therapeutics. Br J Pharmacol 158: 936–946.

Perretti M, Gavins FN (2003). Annexin 1: an endogenous anti-inflammatory protein. News Physiol Sci 18: 60–64.

Perretti M, Getting SJ, Solito E, Murphy PM, Gao JL (2001). Involvement of the receptor for formylated peptides in the in vivo anti-migratory actions of annexin-1 and its mimetics. Am J Pathol 158: 1969–1973.

Sawmynaden P, Perretti M (2006). Glucocorticoid upregulation of the annexin-A1 receptor in leukocytes. Biochem Biophys Res Commun 349: 1351–1355.

Scannell M, Flanagan MB, deStefani A, Wynne KJ, Cagney G, Godson C *et al*. (2007). Annexin-1 and peptide derivatives are released by apoptotic cells and stimulate phagocytosis of apoptotic neutrophils by macrophages. J Immunol 178: 4595–4605.

Serhan CN (2011). The resolution of inflammation: the devil in the flask and in the details. FASEB J 25: 1441–1448.

Singer JP, Chen H, Phelan T, Kukreja J, Golden JA, Blanc PD (2012). Survival following lung transplantation for silicosis and other occupational lung diseases. Occup Med 62: 134–137.

Sudlow AW, Carey F, Forder R, Rothwell NJ (1996). The role of lipocortin-1 in dexamethasone-induced suppression of PGE2 and TNF alpha release from human peripheral blood mononuclear cells. Br J Pharmacol 117: 1449–1456.

Walther A, Riehemann K, Gerke V (2000a). A novel ligand of the formyl peptide receptor: annexin I regulates neutrophil extravasation by interacting with the FPR. Mol Cell 5: 831–840.

Walther A, Riehemann K, Gerke V (2000b). A novel ligand of the formyl peptide receptor: annexin I regulates neutrophil extravasation by interacting with the FPR. Mol Cell 5: 831–840.